EUROPEAN ORGANIZATION FOR NUCLEAR RESEARCH

CERN–PPE/95-43
April 3, 1995

A Search for Lepton Flavour Violating Z^0 Decays

The OPAL Collaboration

Abstract

We have searched for lepton flavour violating $Z^0 \to e\mu$, $Z^0 \to e\tau$ and $Z^0 \to \mu\tau$ decays in a sample of 4.0×10^6 visible Z^0 decays collected with the OPAL detector at LEP during 1991 to 1994. No candidates are found for $Z^0 \to e\mu$. The samples of selected $Z^0 \to e\tau$ and $Z^0 \to \mu\tau$ candidates are consistent with the expected background. The following limits are set at 95% confidence level:

$$\begin{aligned} BR(Z^0 \to e\mu) &< 1.7 \times 10^{-6} \\ BR(Z^0 \to e\tau) &< 9.8 \times 10^{-6} \\ BR(Z^0 \to \mu\tau) &< 17. \times 10^{-6}. \end{aligned}$$

(to be submitted to Zeit. f. Physik)

The OPAL Collaboration

R. Akers[16], G. Alexander[23], J. Allison[16], N. Altekamp[5], K. Ametewee[25], K.J. Anderson[9], S. Anderson[12], S. Arcelli[2], S. Asai[24], D. Axen[29], G. Azuelos[18,a], A.H. Ball[17], E. Barberio[26], R.J. Barlow[16], R. Bartoldus[3], J.R. Batley[5], G. Beaudoin[18], S. Bethke[14], A. Beck[23], G.A. Beck[13], C. Beeston[16], T. Behnke[27], K.W. Bell[20], G. Bella[23], S. Bentvelsen[8], P. Berlich[10], J. Bechtluft[14], O. Biebel[14], I.J. Bloodworth[1], P. Bock[11], H.M. Bosch[11], M. Boutemeur[18], S. Braibant[12], P. Bright-Thomas[25], R.M. Brown[20], A. Buijs[8], H.J. Burckhart[8], R. Bürgin[10], C. Burgard[27], P. Capiluppi[2], R.K. Carnegie[6], A.A. Carter[13], J.R. Carter[5], C.Y. Chang[17], C. Charlesworth[6], D.G. Charlton[1,b], S.L. Chu[4], P.E.L. Clarke[15], J.C. Clayton[1], S.G. Clowes[16], I. Cohen[23], J.E. Conboy[15], O.C. Cooke[16], M. Cuffiani[2], S. Dado[22], C. Dallapiccola[17], G.M. Dallavalle[2], C. Darling[31], S. De Jong[12], L.A. del Pozo[8], H. Deng[17], M.S. Dixit[7], E. do Couto e Silva[12], J.E. Duboscq[8], E. Duchovni[26], G. Duckeck[8], I.P. Duerdoth[16], U.C. Dunwoody[8], J.E.G. Edwards[16], P.G. Estabrooks[6], H.G. Evans[9], F. Fabbri[2], B. Fabbro[21], M. Fanti[2], P. Fath[11], F. Fiedler[12], M. Fierro[2], M. Fincke-Keeler[28], H.M. Fischer[3], R. Folman[26], D.G. Fong[17], M. Foucher[17], H. Fukui[24], A. Fürtjes[8], P. Gagnon[6], A. Gaidot[21], J.W. Gary[4], J. Gascon[18], N.I. Geddes[20], C. Geich-Gimbel[3], S.W. Gensler[9], F.X. Gentit[21], T. Geralis[20], G. Giacomelli[2], P. Giacomelli[4], R. Giacomelli[2], V. Gibson[5], W.R. Gibson[13], J.D. Gillies[20], J. Goldberg[22], D.M. Gingrich[30,a], M.J. Goodrick[5], W. Gorn[4], C. Grandi[2], E. Gross[26], G.G. Hanson[12], M. Hansroul[8], M. Hapke[13], C.K. Hargrove[7], P.A. Hart[9], C. Hartmann[3], M. Hauschild[8], C.M. Hawkes[8], R. Hawkings[8], R.J. Hemingway[6], G. Herten[10], R.D. Heuer[8], J.C. Hill[5], S.J. Hillier[8], T. Hilse[10], P.R. Hobson[25], D. Hochman[26], R.J. Homer[1], A.K. Honma[28,a], R. Howard[29], R.E. Hughes-Jones[16], D.E. Hutchcroft[5], P. Igo-Kemenes[11], D.C. Imrie[25], A. Jawahery[17], P.W. Jeffreys[20], H. Jeremie[18], M. Jimack[1], A. Joly[18], M. Jones[6], R.W.L. Jones[8], P. Jovanovic[1], D. Karlen[6], J. Kanzaki[24], K. Kawagoe[24], T. Kawamoto[24], R.K. Keeler[28], R.G. Kellogg[17], B.W. Kennedy[20], B.J. King[8], J. King[13], J. Kirk[29], S. Kluth[5], T. Kobayashi[24], M. Kobel[10], D.S. Koetke[6], T.P. Kokott[3], S. Komamiya[24], R. Kowalewski[8], T. Kress[11], P. Krieger[6], J. von Krogh[11], P. Kyberd[13], G.D. Lafferty[16], H. Lafoux[8], R. Lahmann[17], W.P. Lai[19], D. Lanske[14], J. Lauber[8], J.G. Layter[4], A.M. Lee[31], E. Lefebvre[18], D. Lellouch[26], J. Letts[2], L. Levinson[26], S.L. Lloyd[13], F.K. Loebinger[16], G.D. Long[17], B. Lorazo[18], M.J. Losty[7], X.C. Lou[8], J. Ludwig[10], A. Luig[10], A. Malik[21], M. Mannelli[8], S. Marcellini[2], C. Markus[3], A.J. Martin[13], J.P. Martin[18], T. Mashimo[24], W. Matthews[25], P. Mättig[3], J. McKenna[29], E.A. Mckigney[15], T.J. McMahon[1], A.I. McNab[13], F. Meijers[8], S. Menke[3], F.S. Merritt[9], H. Mes[7], A. Michelini[8], G. Mikenberg[26], D.J. Miller[15], R. Mir[26], W. Mohr[10], A. Montanari[2], T. Mori[24], M. Morii[24], U. Müller[3], B. Nellen[3], B. Nijjhar[16], S.W. O'Neale[1], F.G. Oakham[7], F. Odorici[2], H.O. Ogren[12], N.J. Oldershaw[16], C.J. Oram[28,a], M.J. Oreglia[9], S. Orito[24], F. Palmonari[2], J.P. Pansart[21], G.N. Patrick[20], M.J. Pearce[1], P.D. Phillips[16], J.E. Pilcher[9], J. Pinfold[30], D.E. Plane[8], P. Poffenberger[28], B. Poli[2], A. Posthaus[3], T.W. Pritchard[13], H. Przysiezniak[30], M.W. Redmond[8], D.L. Rees[1], D. Rigby[1], M.G. Rison[5], S.A. Robins[13], N. Rodning[30], J.M. Roney[28], E. Ros[8], A.M. Rossi[2], M. Rosvick[28], P. Routenburg[30], Y. Rozen[8], K. Runge[10], O. Runolfsson[8], D.R. Rust[12], M. Sasaki[24], C. Sbarra[2], A.D. Schaile[8], O. Schaile[10], F. Scharf[3], P. Scharff-Hansen[8], P. Schenk[4], B. Schmitt[3], M. Schröder[8], H.C. Schultz-Coulon[10], P. Schütz[3], M. Schulz[8], J. Schwiening[3], W.G. Scott[20], M. Settles[12], T.G. Shears[16], B.C. Shen[4], C.H. Shepherd-Themistocleous[7], P. Sherwood[15], G.P. Siroli[2], A. Skillman[15], A. Skuja[17], A.M. Smith[8], T.J. Smith[28], G.A. Snow[17], R. Sobie[28], S. Söldner-Rembold[10], R.W. Springer[30], M. Sproston[20], A. Stahl[3], M. Starks[12], C. Stegmann[10], K. Stephens[16], J. Steuerer[28], B. Stockhausen[3], D. Strom[19], P. Szymanski[20], R. Tafirout[18], P. Taras[18], S. Tarem[26],

M. Tecchio[9], P. Teixeira-Dias[11], N. Tesch[3], M.A. Thomson[8], E. von Törne[3], S. Towers[6], M. Tscheulin[10], T. Tsukamoto[24], A.S. Turcot[9], M.F. Turner-Watson[8], P. Utzat[11], R. Van Kooten[12], G. Vasseur[21], P. Vikas[18], M. Vincter[28], F. Wäckerle[10], A. Wagner[27], D.L. Wagner[9], C.P. Ward[5], D.R. Ward[5], J.J. Ward[15], P.M. Watkins[1], A.T. Watson[1], N.K. Watson[7], P. Weber[6], P.S. Wells[8], N. Wermes[3], B. Wilkens[10], G.W. Wilson[27], J.A. Wilson[1], T. Wlodek[26], G. Wolf[26], S. Wotton[11], T.R. Wyatt[16], G. Yekutieli[26], V. Zacek[18], W. Zeuner[8], G.T. Zorn[17].

[1]School of Physics and Space Research, University of Birmingham, Birmingham B15 2TT, UK
[2]Dipartimento di Fisica dell' Università di Bologna and INFN, I-40126 Bologna, Italy
[3]Physikalisches Institut, Universität Bonn, D-53115 Bonn, Germany
[4]Department of Physics, University of California, Riverside CA 92521, USA
[5]Cavendish Laboratory, Cambridge CB3 0HE, UK
[6]Carleton University, Department of Physics, Colonel By Drive, Ottawa, Ontario K1S 5B6, Canada
[7]Centre for Research in Particle Physics, Carleton University, Ottawa, Ontario K1S 5B6, Canada
[8]CERN, European Organisation for Particle Physics, CH-1211 Geneva 23, Switzerland
[9]Enrico Fermi Institute and Department of Physics, University of Chicago, Chicago IL 60637, USA
[10]Fakultät für Physik, Albert Ludwigs Universität, D-79104 Freiburg, Germany
[11]Physikalisches Institut, Universität Heidelberg, D-69120 Heidelberg, Germany
[12]Indiana University, Department of Physics, Swain Hall West 117, Bloomington IN 47405, USA
[13]Queen Mary and Westfield College, University of London, London E1 4NS, UK
[14]Technische Hochschule Aachen, III Physikalisches Institut, Sommerfeldstrasse 26-28, D-52056 Aachen, Germany
[15]University College London, London WC1E 6BT, UK
[16]Department of Physics, Schuster Laboratory, The University, Manchester M13 9PL, UK
[17]Department of Physics, University of Maryland, College Park, MD 20742, USA
[18]Laboratoire de Physique Nucléaire, Université de Montréal, Montréal, Quebec H3C 3J7, Canada
[19]University of Oregon, Department of Physics, Eugene OR 97403, USA
[20]Rutherford Appleton Laboratory, Chilton, Didcot, Oxfordshire OX11 0QX, UK
[21]CEA, DAPNIA/SPP, CE-Saclay, F-91191 Gif-sur-Yvette, France
[22]Department of Physics, Technion-Israel Institute of Technology, Haifa 32000, Israel
[23]Department of Physics and Astronomy, Tel Aviv University, Tel Aviv 69978, Israel
[24]International Centre for Elementary Particle Physics and Department of Physics, University of Tokyo, Tokyo 113, and Kobe University, Kobe 657, Japan
[25]Brunel University, Uxbridge, Middlesex UB8 3PH, UK
[26]Particle Physics Department, Weizmann Institute of Science, Rehovot 76100, Israel
[27]Universität Hamburg/DESY, II Institut für Experimental Physik, Notkestrasse 85, D-22607 Hamburg, Germany
[28]University of Victoria, Department of Physics, P O Box 3055, Victoria BC V8W 3P6, Canada
[29]University of British Columbia, Department of Physics, Vancouver BC V6T 1Z1, Canada
[30]University of Alberta, Department of Physics, Edmonton AB T6G 2J1, Canada
[31]Duke University, Dept of Physics, Durham, NC 27708-0305, USA

[a] Also at TRIUMF, Vancouver, Canada V6T 2A3
[b] Royal Society University Research Fellow

1 Introduction

There are no strong theoretical arguments to explain the apparent conservation of lepton flavour. The existence of massive neutrinos or the validity of extensions of the Standard Model, for example supersymmetry, could cause flavour changing neutral currents and lepton flavour violation (LFV) in Z^0 decays [1, 2].

All previous searches for lepton flavour violation have reported negative results [3]. Low-q^2 reactions provide stringent constraints on the violation of μ lepton flavour. For example, the 90% c.l. limit on the branching ratio of $\mu \to eee$ of 1.0×10^{-12} [4] can be interpreted as a limit on $BR(Z^0 \to e\mu)$ of 7.4×10^{-13} [1]. Such low-energy limits may not apply, however, in models with q^2-dependent form factors in the interaction.

Searches for neutrinoless τ decays lead to much less stringent limits for the conservation of τ flavour. The CLEO and ARGUS experiments [5] have reported searches for neutrinoless τ decays such as $\tau \to eee$ and $\tau \to \mu\mu\mu$ which imply $BR(Z^0 \to e\tau) < 5.4 \times 10^{-5}$ and $BR(Z^0 \to \mu\tau) < 7.1 \times 10^{-5}$ at 90% c.l. [1]. A direct search for LFV in e^+e^- annihilation at $\sqrt{s} = 29$ GeV has been performed [6], but the measurement is insensitive to LFV arising from couplings to the Z^0 . A direct but statistically limited search for $Z^0 \to e\mu$ in $p\bar{p}$ collision data by the UA1 experiment found no signal [7], resulting in the limit $BR(Z^0 \to e\mu) < 2.2 \times 10^{-3}$ at 90% c.l.. Recent results from the LEP experiments can be found in [8] - [11]. The most stringent 95% c.l. limits, from [11], are: $BR(Z^0 \to e\mu) < 0.6 \times 10^{-5}$, $BR(Z^0 \to e\tau) < 1.3 \times 10^{-5}$ and $BR(Z^0 \to \mu\tau) < 1.9 \times 10^{-5}$.

In this paper we present direct searches for Z^0 decays to $e\mu$, $e\tau$ and $\mu\tau$, within a sample of 4.0×10^6 visible Z^0 decays collected with the OPAL detector at LEP during 1991 to 1994.

2 The OPAL Detector

The OPAL detector, which is described in detail in [12], is a multipurpose apparatus having an acceptance of nearly 4π steradians. The components of the detector relevant for this analysis are briefly described below. A right-handed coordinate system is adopted where the x-axis points to the centre of the LEP ring, and positive z is along the direction of the electron beam. The angles θ and ϕ are the polar and azimuthal angles, respectively.

The trajectories, momenta and energy loss of charged particles are measured in the tracking system, consisting of a silicon micro-vertex detector, a vertex drift chamber and a large volume jet-chamber surrounded by z-chambers which measure charged track coordinates in the direction parallel to the beam axis. The tracking system, under a pressure of 4 bar, is located inside a solenoidal coil which provides a uniform magnetic field of 0.435 Tesla. The jet-chamber measures up to 159 space points between 25.5 cm and 184.5 cm, which can be used to measure the track coordinates and the energy loss. The momentum resolution for 45 GeV muons is 5.3%.

The inactive material in front of the calorimeters, mainly the pressure vessel of the central detector and the coil, amounts to approximately two radiation lengths/$\sin\theta$ for $|\cos\theta| < 0.68$. For the region $|\cos\theta| \geq 0.68$, additional detector material in front of the calorimeters significantly degrades the measured energy resolution. Therefore the analysis is restricted to the barrel region ($|\cos\theta| < 0.68$). The coil is surrounded by a scintillator counter array with 160 azimuthal segments for time-of-flight (TOF) measurement. This is followed by the barrel electromagnetic calorimeter consisting of a presampler in front of a cylindrical array of 9440 lead-glass blocks of 24.6 radiation lengths with pointing geometry. The barrel calorimeter covers $|\cos\theta| < 0.82$. The energy resolution for 45 GeV electrons is 2.5%. The iron return yoke of the magnet is instrumented as a hadron calorimeter, with nine layers of streamer tubes lying parallel to the beam axis, separated by 10-cm thick layers of iron. Inductive strips parallel to each of the 38000 tubes provide muon identification. Muons are also identified in four layers of drift chambers surrounding the hadron calorimeter.

The trigger of the OPAL experiment, possessing substantial redundancy, provides a measured efficiency close to 100% for lepton pairs in the barrel region [13].

3 Overview of the Analysis Procedure

The data were collected in the years 1991 to 1994 at centre of mass energies between 88 GeV and 94 GeV, corresponding to a total integrated luminosity of 129 pb^{-1}.

The event topology for a Z^0 decaying to an unlike pair of leptons (eμ, eτ or $\mu\tau$) is a positively charged lepton (e^+, μ^+ or τ^+) with the beam energy emitted opposite to a negatively charged lepton (e^-, μ^- or τ^-) with a different flavour and also with the beam energy. The τ appears as a highly collimated jet of one or more charged particles, often accompanied by photons. The total visible energy of τ jets is usually significantly less than the beam energy because of undetected neutrinos.

A sample of collinear lepton-pair events is preselected, including events from $Z^0 \rightarrow e^+e^-$, $Z^0 \rightarrow \mu^+\mu^-$ and $Z^0 \rightarrow \tau^+\tau^-$ decays. In this preselection no requirement is made that the lepton flavour on both sides is the same. Only events which contain exactly two charged non-overlapping cones and no neutral cones are considered further. A charged cone consists of charged tracks and electromagnetic clusters [14] within a cone of half-angle 35° and a neutral cone consists of electromagnetic clusters without charged tracks within a cone of the same size [15].

The identification is done for each cone individually by a likelihood method which distinguishes the lepton flavour on the basis of variables such as the number of charged tracks, the number of electromagnetic clusters, matching quality variables, etc. This procedure is described in detail in section 5. Cones which are identified as either an e, μ or τ are then selected by cutting on this 'lepton flavour likelihood' and other discriminating variables. In order to reduce the different background sources in the three search channels, the cuts on these discriminating variables are tuned separately for each search channel using simulated events.

In the search for $Z^0 \rightarrow e\mu$ one cone has to be identified as an electron and the other as a muon. The number of eμ events is extracted from a 2-dimensional distribution of $(E - E_{beam})/\sigma_E$

of the electron candidate versus $(p - p_{beam})/\sigma_p$ of the muon candidate, where E denotes the total electromagnetic cone energy of the electron candidate, σ_E its error, p the total charged track cone momentum for the muon candidate and σ_p its error. In this channel the dominant background comes from $Z^0 \to \tau^+\tau^-$ events, where one τ decays to an electron and the other to a muon.

Events consisting of an identified electron cone and an identified τ cone are candidates for the $Z^0 \to e\tau$ search. Apart from possible $Z^0 \to e\tau$ decays this sample contains events mainly from $Z^0 \to \tau^+\tau^-$ where one τ decays to an electron and a small fraction from $Z^0 \to e^+e^-$ events with one electron misidentified. The energy spectrum of the electron candidates is used for extracting the number of events from $Z^0 \to e\tau$. Electrons from $Z^0 \to e\tau$ events would have the beam energy, whereas electron candidates from $Z^0 \to \tau^+\tau^-$ events have a broad spectrum. A sum of these distributions is fitted to the observed spectrum using a likelihood fit. The 95% confidence level limit is derived from the integration of the likelihood function.

The search in the $\mu\tau$ channel is similar to the $e\tau$ search, but with the fit now applied to the momentum spectrum of the muon candidates. Apart from possible $Z^0 \to \mu\tau$ decays the $\mu\tau$ sample contains events mainly from $Z^0 \to \tau^+\tau^-$ and a small fraction from $Z^0 \to \mu^+\mu^-$ events with one muon misidentified.

The 95% confidence level limits on each of the lepton flavour violating branching ratios are obtained by correcting for the event selection efficiencies and normalizing to the measured decay rate of $Z^0 \to \mu^+\mu^-$. Systematic uncertainties in the analysis are included in the calculation.

4 Preselection of Lepton Pairs

Lepton pair candidates are preselected from a sample of events satisfying the preselection cuts described in [13] and [15]. To reject background events arising from cosmic rays and two-photon events some additional cuts [14] are made. Events are further required to satisfy the following conditions:

- the polar angles θ_i of both cones satisfy $|\cos\theta_i| < 0.68$, where the direction of the cone is calculated from the momentum sum of the charged tracks and the energy sum of the clusters in the cone
- exactly two charged cones are found
- no neutral cones are found
- the acollinearity angle between the axes of the two cones must be less than 10°
- no energy measured in the forward detectors.

The lepton pair preselection efficiencies for events within $|\cos\theta_i| < 0.68$, determined using $Z^0 \to e^+e^-$, $Z^0 \to \mu^+\mu^-$ and $Z^0 \to \tau^+\tau^-$ Monte Carlo events, are $(90.16 \pm 0.02)\%$ for $Z^0 \to e^+e^-$, $(92.38 \pm 0.01)\%$ for $Z^0 \to \mu^+\mu^-$ and $(87.58 \pm 0.01)\%$ for $Z^0 \to \tau^+\tau^-$events (only statistical errors are given). These preselection efficiencies have been checked with data and the systematic errors are approximately 0.1%.

5 Lepton Identification

Leptons are identified by means of a likelihood method. Suitable variables to separate the different lepton species are chosen (see below). The measured values of the variables are compared to properly normalized reference distributions. For the identification of simulated events reference distributions from Monte Carlo events are used, while for the identification of the data, reference distributions from tagged data events are taken.

Two examples from Monte Carlo events are shown in fig. 1. For the simulation we use the Monte Carlo program BABAMC 2.0 [16] for $Z^0 \rightarrow e^+e^-$ events, KORALZ 3.8 and 4.0 [17] for $Z^0 \rightarrow \mu^+\mu^-$ events and for τ production and TAUOLA 1.5 and 2.4 [18] for τ decays. The detector is simulated using OPAL's GEANT-based program [19].

To obtain the data reference distributions it is necessary to get tagged samples of $Z^0 \rightarrow e^+e^-$, $Z^0 \rightarrow \mu^+\mu^-$ and $Z^0 \rightarrow \tau^+\tau^-$ events from data with high purity. These event samples were tagged by making stringent cuts on the likelihood weights, evaluated using the Monte Carlo reference distributions, as well as cuts on the total electromagnetic cone energy divided by the beam energy and the total charged track cone momentum divided by the beam momentum. In each event one cone is clearly identified as an electron, muon or τ, respectively, and the opposite cones were then available as relatively unbiased test samples of electron, muon or τ cones. Note that these test samples would also include LFV events. The impurities from wrong lepton pair species are measured to be less than 0.1%.

These tagged event samples from data are also used for cross checks of the background shapes calculated from $Z^0 \rightarrow \tau^+\tau^-$ Monte Carlo events and to derive the efficiencies of the lepton cone identification from data. In addition all reference distributions taken from simulated events have been checked against the data distributions of tagged lepton pair events (fig. 2).

The differences arising from the use of the Monte Carlo reference distributions for the identification of Monte Carlo events and of the data reference distributions to identify the data do not influence the limits derived in this analysis, since the selection efficiencies are calculated largely from the tagged data event samples. As an exception, for the $\mu\tau$ channel, τ reference distributions from Monte Carlo events have been used where $\tau \rightarrow \mu\nu\bar{\nu}$ decays are excluded to avoid misidentification of $Z^0 \rightarrow \mu^+\mu^-$ events where one muon is misidentified as a τ. This significantly improves the separation between muon and τ cones.

The weight $w_i^j(x_i)$ that a cone was formed by a lepton of species $j = e, \mu, \tau$, based on the distribution of the likelihood variable $i = 1, N_{\rm var}$ with the measured value x_i, is given by:

$$w_i^j(x_i) \;=\; \frac{f_i^j(x_i)}{\sum\limits_{j=e,\mu,\tau} f_i^j(x_i)} \quad , \tag{1}$$

where $f_i^j(x_i)$ is the normalized weight function given by the corresponding reference distribution. The combined lepton flavour likelihood weights $\mathcal{L}^j(x)$ are formed by multiplying the $w_i^j(x_i)$ obtained for each of the $N_{\rm var}$ likelihood variables. After normalizing, one gets:

$$\mathcal{L}^j(x) \;=\; \frac{\prod_{i=1}^{N_{\rm var}} w_i^j(x_i)}{\sum\limits_{j={\rm e},\mu,\tau}\left(\prod_{i=1}^{N_{\rm var}} w_i^j(x_i)\right)} \quad . \tag{2}$$

The distributions for the resulting likelihood weights for the different Monte Carlo channels ($Z^0\rightarrow e^+e^-$, $Z^0\rightarrow \mu^+\mu^-$ and $Z^0\rightarrow \tau^+\tau^-$) are shown in figs. 3a - 3c.

The most important **cone** variables which are used for the likelihood identification are listed below.

For separation between all three lepton species:

- the total electromagnetic cone energy divided by the beam energy (x_E)
- the electromagnetic energy associated to the track with highest momentum divided by its momentum (E/p)

For separation of μ from e or τ:

- the number of hits in the last 3 layers of the hadron calorimeter and the 4 layers of the muon chamber
- the weight for the matching of the charged track with the nearest reconstructed track in the muon chambers

For separation of τ from e or μ:

- the total charged track cone momentum divided by the beam momentum (x_p)

For separation of e and μ:

- the average number of strips hit per layer of the hadron calorimeter

Because the variables x_E and x_p are strongly correlated to the variables from which the limits are extracted in the next sections they have been used as a likelihood variable only for the identification of τ cones.

6 Selection of $Z^0\rightarrow e\mu$ Candidates

The following criteria are optimized to identify the cones as electron and muon, respectively, and to suppress background, mainly from $Z^0\rightarrow \tau^+\tau^-$ events:

- electron cone identification
  - the electron likelihood weight must be greater than 80% and the τ likelihood weight less than 4%
  - the total charged track cone momentum must be greater than 10% of the beam momentum, to suppress background from radiative $Z^0 \rightarrow \mu^+\mu^-$ events
  - the relative error on the total electromagnetic cone energy (σ_E/E) must be less than 6%
- muon cone identification
  - the muon likelihood weight must be greater than 90%
  - the relative error on the total charged track cone momentum (σ_p/p) must be less than 15%.

The efficiency for selecting electron candidates from the preselected sample is measured to be $(77.7 \pm 1.0)\%$, while for muon candidates it is $(94.1 \pm 1.0)\%$. The errors given are the systematic errors determined in section 9.

Fig. 4 shows the final 2-dimensional distribution of $(E - E_{beam})/\sigma_E$ for the electron candidate versus $(p - p_{beam})/\sigma_p$ for the muon candidate, for $Z^0 \rightarrow \tau^+\tau^-$ Monte Carlo and data. The signal region is defined to be the region within 3 standard deviations. Fig. 4a shows the distribution for the expected background from $Z^0 \rightarrow \tau^+\tau^-$ Monte Carlo events with the same cuts applied. We found two events from the $Z^0 \rightarrow \tau^+\tau^-$ Monte Carlo in the signal region which corresponds, after normalization to data, to 0.6 expected events. No events from $Z^0 \rightarrow e^+e^-$ and $Z^0 \rightarrow \mu^+\mu^-$ Monte Carlo were found inside the plotted region shown in fig. 4. In the data distribution (fig. 4b) we find no events within 3 standard deviations of the expected signal, resulting in a 95% c.l. upper limit $N_{e\mu}$ of 3.0 events for a possible contribution from $Z^0 \rightarrow e\mu$ decays.

7 Selection of $Z^0 \rightarrow e\tau$ Candidates

The following criteria are optimized to identify the cones as electron and τ, respectively and to suppress the background, here from $Z^0 \rightarrow e^+e^-$ and $Z^0 \rightarrow \tau^+\tau^-$ decays:

- electron cone identification
  - the electron likelihood weight must be greater than 95%
  - the total charged track cone momentum must be greater than 15% of the beam momentum
  - the total cone energy which is not associated to the track with highest momentum divided by the beam energy (E_{else}/E_{beam}) must be less than 0.9
  - the centre of gravity of the most energetic electromagnetic cluster must point to a lead glass block which has been properly calibrated with e^+e^- events

- the relative error on the total electromagnetic cone energy (σ_E/E) must be less than 6%

- τ cone identification

  - the τ likelihood weight must be greater than 99.5% and the electron likelihood weight must be less than 10^{-5}
  - the total electromagnetic cone energy must be less than 70% of the beam energy
  - the total charged track cone momentum must be less than 70% of the beam momentum
  - E_{else}/E_{beam} must be less than 0.2
  - the track with the highest momentum must not be identified as an electron by the measurement of the energy loss ($\mathrm{d}E/\mathrm{d}x$) and momentum in the jet-chamber.

The efficiency for selecting electron candidates according to these requirements is measured to be $(68.4 \pm 1.0)\%$, while the efficiency for selecting τ candidates is $(30.9 \pm 1.0)\%$.

Fig. 5a shows the total electromagnetic cone energy divided by the beam energy, x_E, of the electron candidates after all cuts. The dots represent the measured distribution from data, the histogram shows the Monte Carlo distribution for $\mathrm{Z}^0 \to \tau^+\tau^-$ events, normalized to the data. Of this predicted $\mathrm{Z}^0 \to \tau^+\tau^-$ background 95% comes from the decay $\tau \to e\nu\bar{\nu}$. The dashed histogram shows the shape of the expected signal. This distribution has been obtained from tagged $\mathrm{Z}^0 \to \mathrm{e}^+\mathrm{e}^-$ data events after applying the electron cone identification cuts. From the $\mathrm{Z}^0 \to \mathrm{e}^+\mathrm{e}^-$ Monte Carlo we expect 4.1 ± 1.7 background events in the whole data spectrum of x_E. No events from the $\mathrm{Z}^0 \to \mu^+\mu^-$ Monte Carlo passed the $\mathrm{Z}^0 \to \mathrm{e}\tau$ selection cuts described above.

To calculate the size of the signal the sum of the x_E distributions from $\mathrm{Z}^0 \to \tau^+\tau^-$ Monte Carlo events and of the expected signal from tagged $\mathrm{Z}^0 \to \mathrm{e}^+\mathrm{e}^-$ data events and of the fixed scaled background from $\mathrm{Z}^0 \to \mathrm{e}^+\mathrm{e}^-$ Monte Carlo events are fitted to the data distribution. This is done considering the statistical error of the data and the Monte Carlo distributions [21]. The likelihood probability as a function of the number of signal events, shown in fig. 6, is calculated. The integration of the likelihood function yields a 95% c.l. upper limit $N_{\mathrm{e}\tau}$ of 5.0 events (see section 9) on a possible contribution from $\mathrm{Z}^0 \to \mathrm{e}\tau$ decays. Fig. 5b shows the interesting region around $x_E = 1.0$ and, in addition, the dotted histogram of the predicted $\mathrm{Z}^0 \to \tau^+\tau^-$ background plus the 95% c.l. signal.

8 Selection of $\mathrm{Z}^0 \to \mu\tau$ Candidates

In searching for $\mathrm{Z}^0 \to \mu\tau$ we require one cone to be identified as a muon and the other as a τ decay. The following criteria must also be met to suppress the background from $\mathrm{Z}^0 \to \mu^+\mu^-$ and $\mathrm{Z}^0 \to \tau^+\tau^-$ decays:

- muon cone identification
  - the muon likelihood weight must be greater than 99%
  - the barrel muon chambers must have at least one hit associated with the charged track of the muon candidate
  - to ensure a good momentum resolution the relative error on the total charged track cone momentum (σ_p/p) must be less than 6.5% for the data from 1991 and 1992 and less than 7.0% for the data from 1993 and 1994, depending on the data quality
- τ cone identification
  - the τ likelihood weight must be greater than 90% and the muon likelihood weight must be less than 10^{-6}
  - no associated hits in the barrel muon chambers
  - the total charged track cone momentum must be greater than 2% and less than 95% of the beam momentum
  - E_{else}/E_{beam} must be equal to 0 or greater than 0.02
  - the sum of x_E and x_p must be less than 0.95 or greater than 1.1.

The efficiency for selecting muon candidates according to these requirements is measured to be $(55.1 \pm 1.0)\%$. For selecting τ candidates we find $(44.7 \pm 1.0)\%$.

Fig. 7a shows the total charged track cone momentum divided by the beam momentum, x_p, of the muon candidates after all cuts. The dots represent the measured distribution from data and the histogram shows the distribution from $Z^0 \rightarrow \tau^+\tau^-$ Monte Carlo events, normalized to the data. Of this predicted $Z^0 \rightarrow \tau^+\tau^-$ background 90% comes from the decay $\tau \rightarrow \mu\nu\bar{\nu}$. The dashed histogram shows the shape of the expected signal. This distribution has been obtained from tagged $Z^0 \rightarrow \mu^+\mu^-$ data events after applying the muon cone identification cuts. No events from the $Z^0 \rightarrow e^+e^-$ Monte Carlo passed the $Z^0 \rightarrow \mu\tau$ selection cuts described above. From the $Z^0 \rightarrow \mu^+\mu^-$ Monte Carlo we expect 4.2 ± 1.2 background events in the whole data spectrum of x_p.

The extraction of the limits for the $Z^0 \rightarrow \mu\tau$ channel is similar to that for $Z^0 \rightarrow e\tau$. To calculate the size of the signal the sum of the x_p distributions from $Z^0 \rightarrow \tau^+\tau^-$ Monte Carlo events and of the expected signal from tagged $Z^0 \rightarrow \mu^+\mu^-$ data events and of the fixed scaled background from $Z^0 \rightarrow \mu^+\mu^-$ Monte Carlo events are fitted to the data distribution. This is done considering the statistical error of the data and the Monte Carlo distributions [21]. The likelihood probability as a function of the number of signal events, shown in fig. 8, is calculated. The integration of the likelihood function yields a 95% c.l. upper limit $N_{\mu\tau}$ of 9.9 events (see section 9) on a possible contribution from $Z^0 \rightarrow \mu\tau$ decays. Fig. 7b shows the interesting region around $x_p = 1.0$ and, in addition, the dotted histogram of the predicted $Z^0 \rightarrow \tau^+\tau^-$ background plus the 95% c.l. signal.

9 Systematic Studies and Efficiency Calculation

Likelihood identification
All likelihood reference distributions obtained using Monte Carlo events have been checked with tagged data events. Examples of these comparisons are shown in fig. 2. The agreement was found to be good but with some discrepancies. For the likelihood identification of the data the reference distributions from tagged data events are used, except for the $\mu\tau$ channel where τ reference distributions from Monte Carlo events without $\tau \to \mu\nu\bar{\nu}$ decays are used. The τ reference distributions including all τ decays from Monte Carlo events have been checked with tagged data events. No significant differences have been found.

Systematic studies on the fitting procedure
The $Z^0 \to e\tau$ and $Z^0 \to \mu\tau$ limits were recalculated using several different binnings of the x_E and x_p distributions, respectively. The variations in the calculated limits were found to be small, as shown in table 1. The x_E and x_p intervals of the fits have also been varied. These changes give no significant difference in the fit results.

	40 bins	50 bins	60 bins	70 bins	80 bins	90 bins	mean
$e\tau$ 95% c.l. limit	5.1	4.9	4.8	5.1	5.0	4.9	5.0
$\mu\tau$ 95% c.l. limit	10.0	9.7	9.7	10.1	10.1	10.0	9.9

Table 1: *95% c.l. limits for the* $e\tau$ *and* $\mu\tau$ *channels, using different bin widths.*

The mean values are used for the final calculation of the 95% c.l. limits on the branching ratios. 95% c.l. limits of 5.0 events in the $e\tau$ channel and of 9.9 events in the $\mu\tau$ channel are found.

Check of the τ spectra
The shapes of the x_E distribution (fig. 9a) and of the x_p distribution (fig. 9b) of τ cones from Monte Carlo events have been checked with tagged data events. No significant differences have been found which would influence the limits obtained by using the Monte Carlo τ spectra.

Efficiency calculation

- **Preselection efficiencies**
  The lepton pair preselection efficiencies in the region $|\cos\theta_i| < 0.68$ are given in section 4. Preselection efficiencies for LFV events (κ_{xy}) would be expected to lie between those for the corresponding like-flavour lepton pair events (κ_{xx} and κ_{yy}). This assumption has been checked in a similar analysis. To be conservative in our calculation of the limits we use the lower limits for the preselection efficiencies: $\kappa_{e\mu} = (90.2 \pm 0.1)\%$, $\kappa_{e\tau} = (87.6 \pm 0.1)\%$ and $\kappa_{\mu\tau} = (87.6 \pm 0.1)\%$.

- **Lepton identification efficiencies**
  The efficiencies, after the preselection, measured in data with tagged events compared to Monte Carlo with and without applying the tagging requirements are given in table 2.

  The agreement between the tagged data and tagged Monte Carlo samples is satisfactory with the exception of the τ identification in the $e\tau$ channel. This difference comes from

channel	ID	DATA tagged	MC tagged	MC	efficiencies
eμ	e	76.7 ± 0.1	77.9 ± 0.1	79.0 ± 0.1	77.7 ± 1.0
eμ	μ	94.7 ± 0.1	94.7 ± 0.1	94.1 ± 0.1	94.1 ± 1.0
eτ	e	67.6 ± 0.1	67.0 ± 0.1	67.7 ± 0.1	68.4 ± 1.0
eτ	τ	31.4 ± 0.2	34.1 ± 0.1	33.6 ± 0.1	30.9 ± 1.0
$\mu\tau$	μ	56.4 ± 0.1	56.7 ± 0.1	55.4 ± 0.1	55.1 ± 1.0
$\mu\tau$	τ	44.8 ± 0.2	44.4 ± 0.1	44.3 ± 0.1	44.7 ± 1.0

Table 2: *Lepton identification efficiencies in %.*

the stringent requirement on the electron likelihood weight. The selection efficiencies from the tagged data events are corrected for the small bias introduced by the tagging procedure. This bias is calculated using Monte Carlo events and is less than 1% (compare column 'MC' and 'MC tagged' of table 2). This bias is taken as the systematic uncertainty of the lepton identification efficiencies. The final corrected efficiencies are given in the 'efficiencies' column of table 2.

10 Limits on Z^0 Branching Ratios

In calculating limits on the lepton flavour violating Z^0 branching ratios, the 95% c.l. limits on the numbers of signal events N_{xy} must be corrected for preselection efficiencies κ_{xy} and lepton identification efficiencies ε_x and ε_y. The numbers used for the limit calculations are summarized in table 3.

$channel_{xy}$	N_{xy}	κ_{xy} [%]	ε_x [%]	ε_y [%]
eμ	3.0	90.2 ± 0.1	77.7 ± 1.0	94.1 ± 1.0
eτ	5.0	87.6 ± 0.1	68.4 ± 1.0	30.9 ± 1.0
$\mu\tau$	9.9	87.6 ± 0.1	55.1 ± 1.0	44.7 ± 1.0

Table 3: *Summary of numbers for the calculation of the limits.*

Normalizing N_{xy} to the number of produced Z^0 N_{Z^0} in the same data sample one finds:

$$BR(Z^0 \to xy) < \frac{N_{xy}}{\varepsilon_x \cdot \varepsilon_y \cdot \kappa_{xy}} \cdot \frac{1}{N_{Z^0}} \quad , \tag{3}$$

where $N_{Z^0} = 2.748 \times 10^6$ is calculated from the identified $Z^0 \to \mu^+\mu^-$ events [15] inside $|\cos\theta| < 0.68$, corrected for efficiency and branching ratio [3]. Considering error propagation and incorporating all systematic uncertainties into the limits [22] we obtain the following final limits at the 95% confidence level:

$$BR(Z^0 \to e\mu) < 1.7 \times 10^{-6}, BR(Z^0 \to e\tau) < 9.8 \times 10^{-6}, BR(Z^0 \to \mu\tau) < 17. \times 10^{-6}.$$

11 Conclusion

No evidence for lepton flavour violating Z^0 decays is found in any of the three searches described in this paper. No candidate events are found in the $Z^0 \to e\mu$ channel. The observed candidates in the eτ and $\mu\tau$ channels are consistent with the expected background. The following limits at the 95% confidence level have been found:

$$\begin{aligned} BR(Z^0 \to e\mu) &< 1.7 \times 10^{-6} \\ BR(Z^0 \to e\tau) &< 9.8 \times 10^{-6} \\ BR(Z^0 \to \mu\tau) &< 17. \times 10^{-6}. \end{aligned}$$

To obtain the limits on the branching ratios we made the usual assumption that the $Z^0 \to xy$ (with x,y an unlike pairing of e, μ or τ) events have the same angular distribution as the $Z^0 \to \mu^+\mu^-$ events. Although we quote limits on $Z^0 \to xy$ no assumption has been made that the final state is produced via a Z^0 boson. Therefore, the limits apply equally well to any reaction $e^+e^- \to xy$.

12 Acknowledgements

It is a pleasure to thank the SL Division for the efficient operation of the LEP accelerator, the precise information on the absolute energy, and their continuing close cooperation with our experimental group. In addition to the support staff at our own institutions we are pleased to acknowledge the
Department of Energy, USA,
National Science Foundation, USA,
Particle Physics and Astronomy Research Council, UK,
Natural Sciences and Engineering Research Council, Canada,
Fussefeld Foundation,
Israel Ministry of Science,
Israel Science Foundation, administered by the Israel Academy of Science and Humanities,
Minerva Gesellschaft,
Japanese Ministry of Education, Science and Culture (the Monbusho) and a grant under the Monbusho International Science Research Program,
German Israeli Bi-national Science Foundation (GIF),
Direction des Sciences de la Matière du Commissariat à l'Energie Atomique, France,
Bundesministerium für Forschung und Technologie, Germany,
National Research Council of Canada,
A.P. Sloan Foundation and Junta Nacional de Investigação Científica e Tecnológica, Portugal.

References

[1] For an overview and further references see:
E.W.N. Glover, J.J. van der Bij in Z Physics at LEP 1,
eds. G. Altarelli, R. Kleiss, C. Verzegnassi, CERN 89-08 Vol. 2 (1989) 34;
J.W.F. Valle, Prog. Part. Nucl. Phys. **26** (1991) 91.

[2] T.K. Kuo and N. Nakagawa, Phys. Rev. **D32** (1985) 306;
J. Bernabeu *et al.*, Phys. Lett. **B187** (1987) 303;
G. Eilam and T.G. Rizzo, Phys. Lett. **B188** (1987) 91;
M.J.S. Levine, Phys Rev. **D36** (1987) 1329;
J. Bernabeu and A. Santamaria, Phys. Lett. **B197** (1987) 418;
C.A. Heusch *et al.*, Nucl. Phys. **B416** (1994) 3.

[3] Particle Data Group, Phys. Rev. **D50** (1994) 1173.

[4] Sindrum Collaboration, U. Bellgardt *et al.*, Nucl. Phys. **B299** (1988) 1.

[5] ARGUS Collaboration, H. Albrecht *et al.*, Z. Phys. **C55** (1992) 179;
CLEO Collaboration, T. Bowcock *et al.*, Phys. Rev. **D41** (1990) 805.

[6] MARK II Collaboration, J.J. Gomez-Cadenas *et al.*, Phys. Rev. Lett. **66** (1991) 1007.

[7] UA1 Collaboration, C. Albajar *et al.*, Z. Phys. **C44** (1989) 15.

[8] OPAL Collaboration, M.Z. Akrawy *et al.*, Phys. Lett. **B254** (1991) 293.

[9] ALEPH Collaboration, D. Decamp *et al.*, Phys. Rep. **216** (1992) 253.

[10] DELPHI Collaboration, P. Abreu *et al.*, Phys. Lett. **B298** (1992) 247.

[11] L3 Collaboration, O. Adriani *et al.*, Phys. Lett. **B316** (1993) 427.

[12] OPAL Collaboration, K. Ahmet *et al.*, Nucl. Instr. and Meth. **A305** (1991) 275;
P.P. Allport *et al.*, Nucl. Instr. and Meth. **A324** (1993) 34;
P.P. Allport *et al.*, Nucl. Instr. and Meth. **A346** (1994) 476.

[13] OPAL Collaboration, M.Z. Akrawy *et al.*, Phys. Lett. **B247** (1990) 458;
M. Arignon *et al.*, Nucl. Instr. and Meth. **A313** (1992) 103.

[14] OPAL Collaboration, G. Alexander *et al.*, Phys. Lett. **B266** (1991) 201.

[15] OPAL Collaboration, G. Alexander *et al.*, Z. Phys. **C52** (1991) 175.

[16] F.A. Berends *et al.*, Nucl. Phys. **B304** (1988) 712.

[17] S. Jadach *et al.*, Comp. Phys. Comm. **66** (1991) 276;
S. Jadach *et al.*, Comp. Phys. Comm. **79** (1994) 503.

[18] S. Jadach *et al.*, Comp. Phys. Comm. **64** (1991) 275;
S. Jadach *et al.*, Comp. Phys. Comm. **76** (1993) 361.

[19] J. Allison *et al.*, Comp. Phys. Comm. **47** (1987) 171;
J. Allison *et al.*, Nucl. Instr. and Meth. **A317** (1992) 47.

[20] O. Biebel *et al.*, Nucl. Instr. and Meth. **A323** (1992) 169.

[21] R. Barlow, C. Beeston, Comp. Phys. Comm. **77** (1993) 219.

[22] R. D. Cousins, V. L. Highland, Nucl. Instr. and Meth. **A320** (1992) 331.

Fig. 1

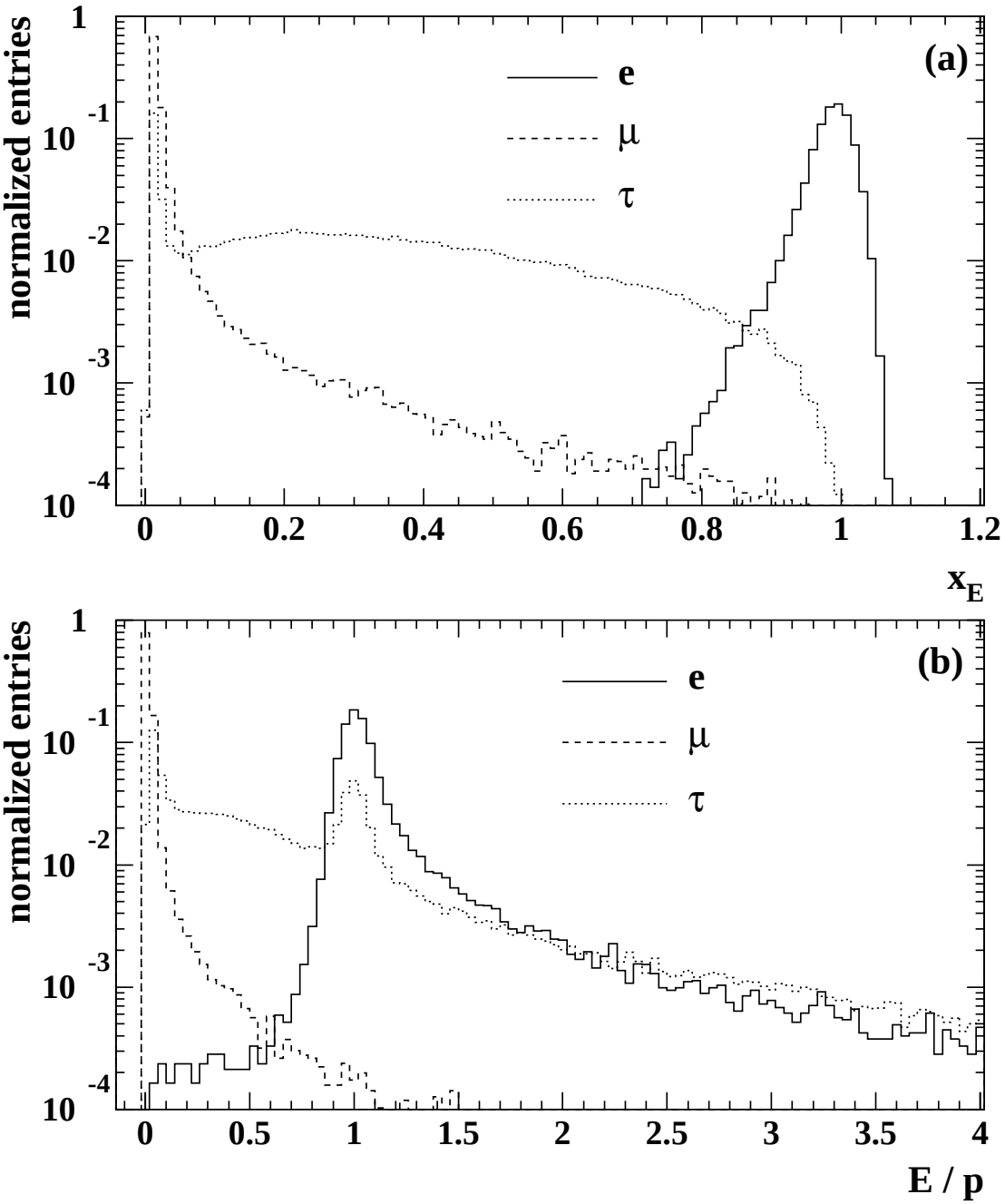

Figure 1: *Reference distributions of the variables x_E (a) and E/p (b), determined from* $Z^0 \to e^+e^-$, $Z^0 \to \mu^+\mu^-$ *and* $Z^0 \to \tau^+\tau^-$ *Monte Carlo events.*

Fig. 2

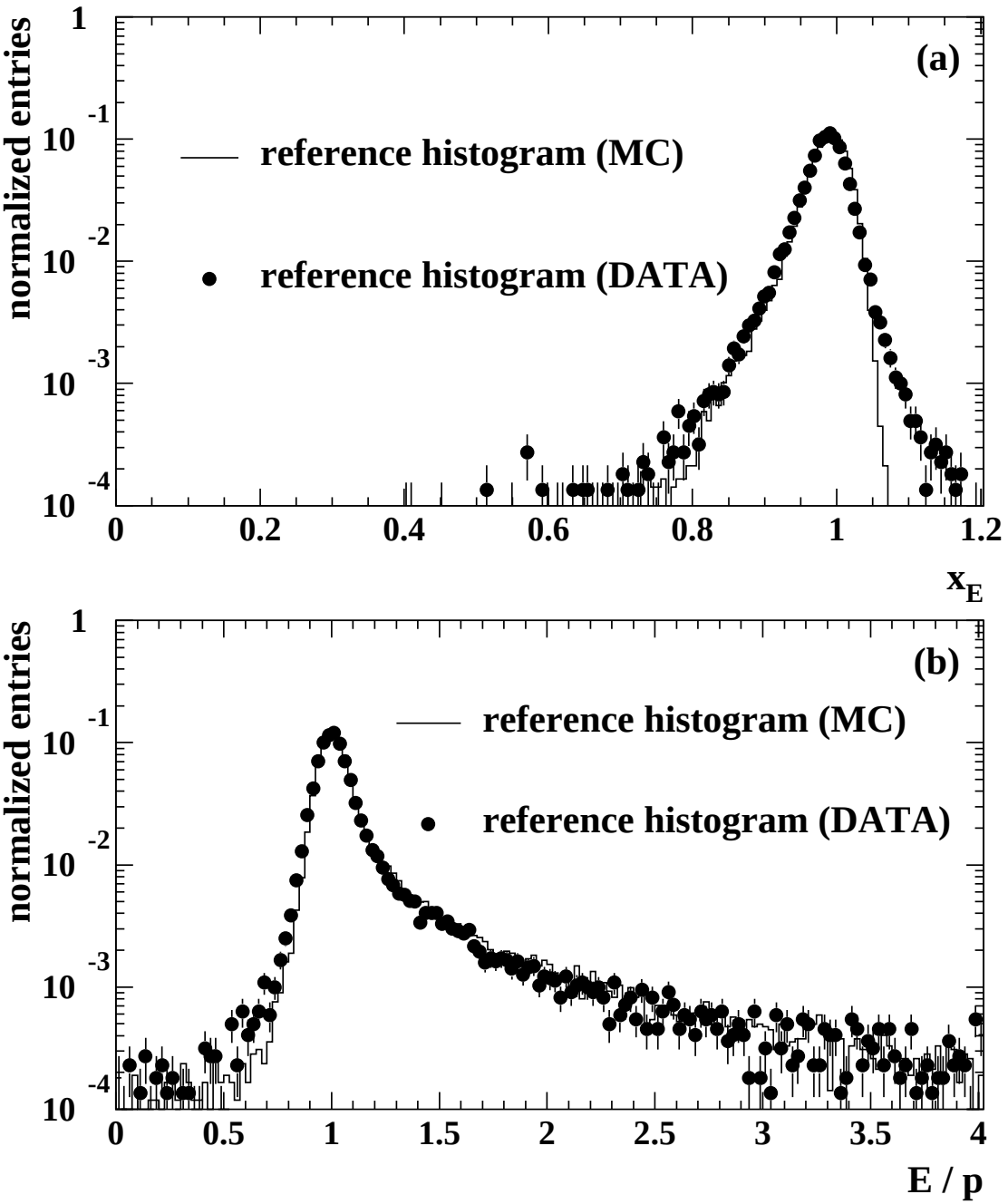

Figure 2: *Reference distributions of the variables x_E (a) and E/p (b) for* $Z^0 \rightarrow e^+e^-$ *events, determined from Monte Carlo (histograms) and from tagged data events (dots).*

Fig. 3

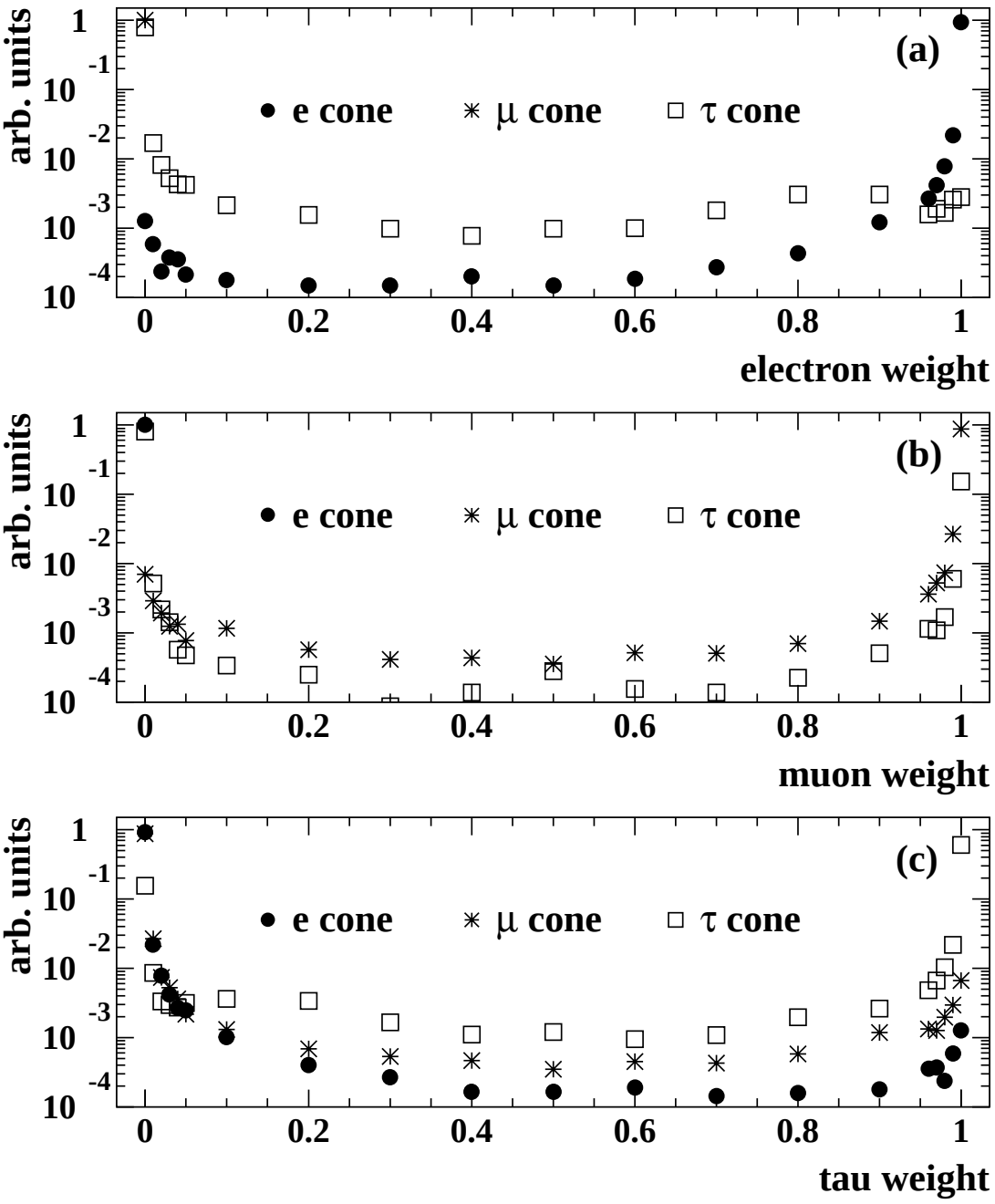

Figure 3: *Likelihood weights for* $Z^0 \rightarrow e^+e^-$, $Z^0 \rightarrow \mu^+\mu^-$ *and* $Z^0 \rightarrow \tau^+\tau^-$ *Monte Carlo samples. Predicted distributions of electron (a), muon (b) and* τ *(c) likelihood weights for each of the three lepton species.*

Fig. 4

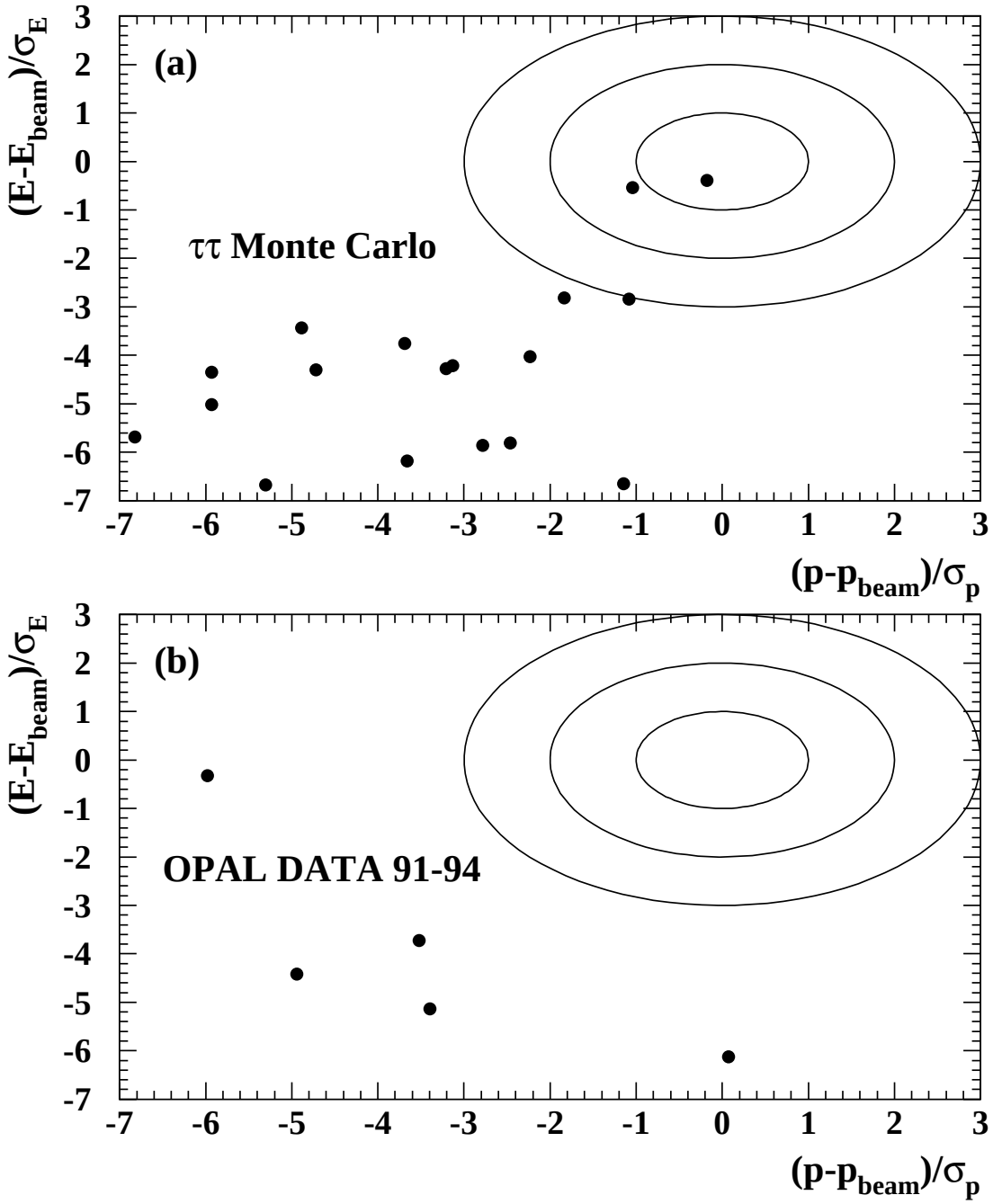

Figure 4: *Difference between the total electromagnetic cone energy of the electron candidates and the beam energy divided by the error on the energy versus the difference between the total charged track cone momentum of the muon candidates and the beam momentum divided by the error on the momentum after the cuts for the* eμ *selection described in the text. Shown are the one, two and three standard deviation contours. In (a) the distribution from* $Z^0 \rightarrow \tau^+\tau^-$ *Monte Carlo events, with 3.6 times the data statistics, is shown and in (b) the data distribution.*

Fig. 5

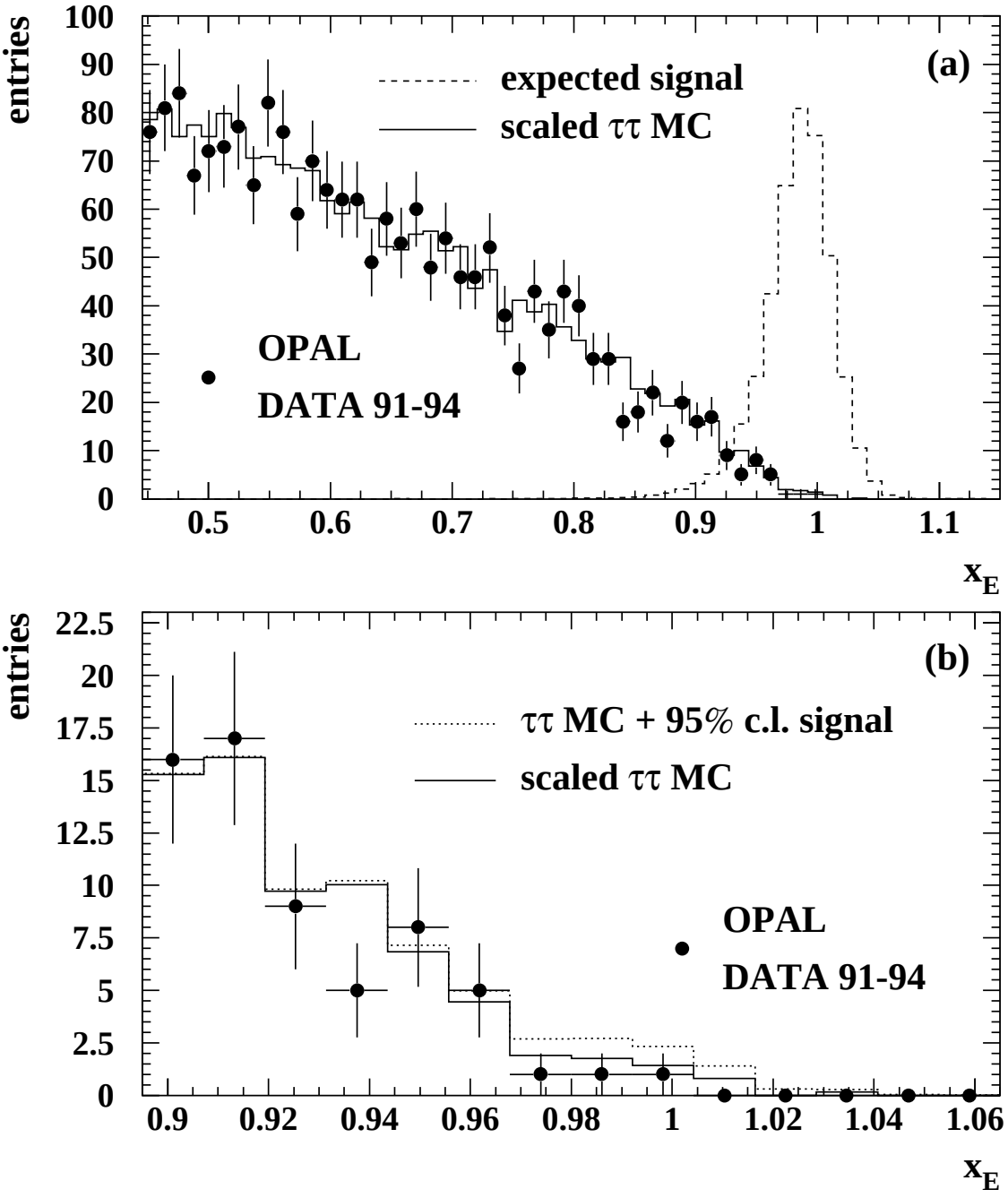

Figure 5: *Distribution of x_E of the electron candidates after all cuts for the eτ selection in data (dots), in $Z^0 \rightarrow \tau^+\tau^-$ Monte Carlo (histogram) and the shape of the expected signal of electron cones from tagged $Z^0 \rightarrow e^+e^-$ data events (dashed line). In (a) the entire x_E distribution is shown, while in (b) the interesting region around $x_E = 1$ is shown. The level of the signal shape is arbitrary in (a), while in (b) the $Z^0 \rightarrow \tau^+\tau^-$ Monte Carlo plus the 95% c.l. signal is shown as the dotted histogram.*

Fig. 6

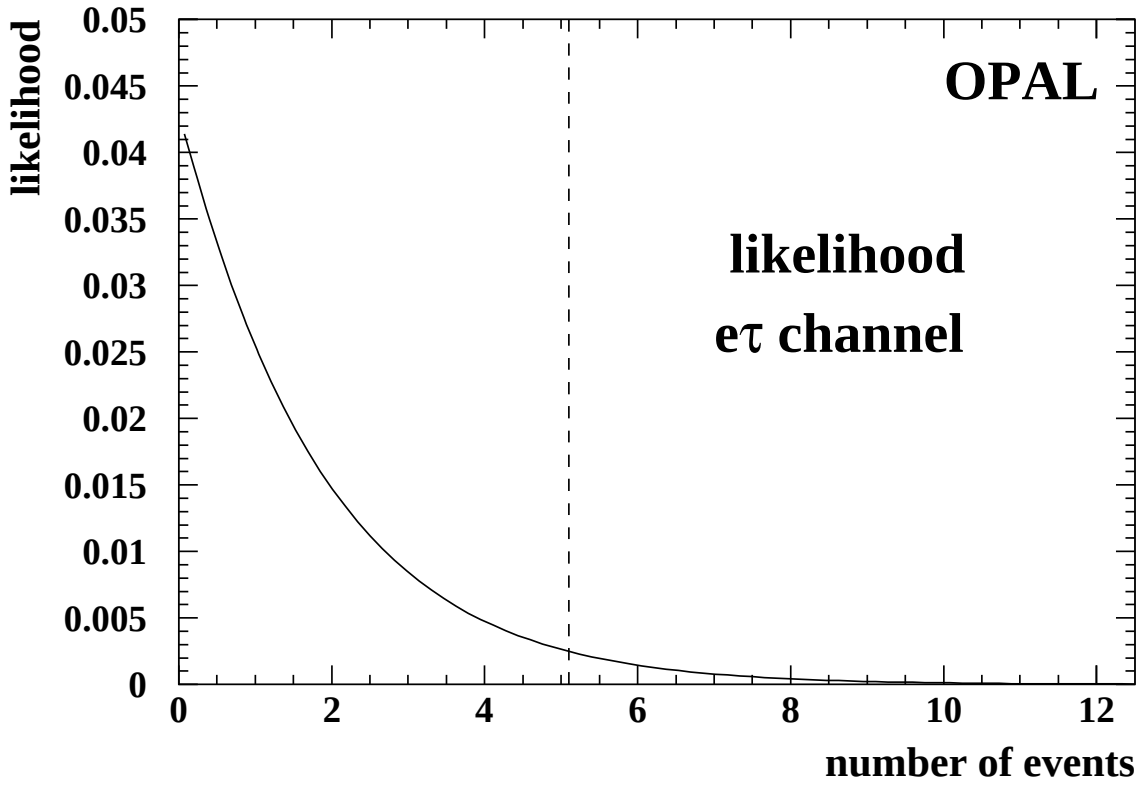

Figure 6: *Likelihood as a function of the number of* $e\tau$ *events in the data sample for 70 bins. The dashed line corresponds to the 95% c.l. limit on the number of* $Z^0 \rightarrow e\tau$ *events.*

Fig. 7

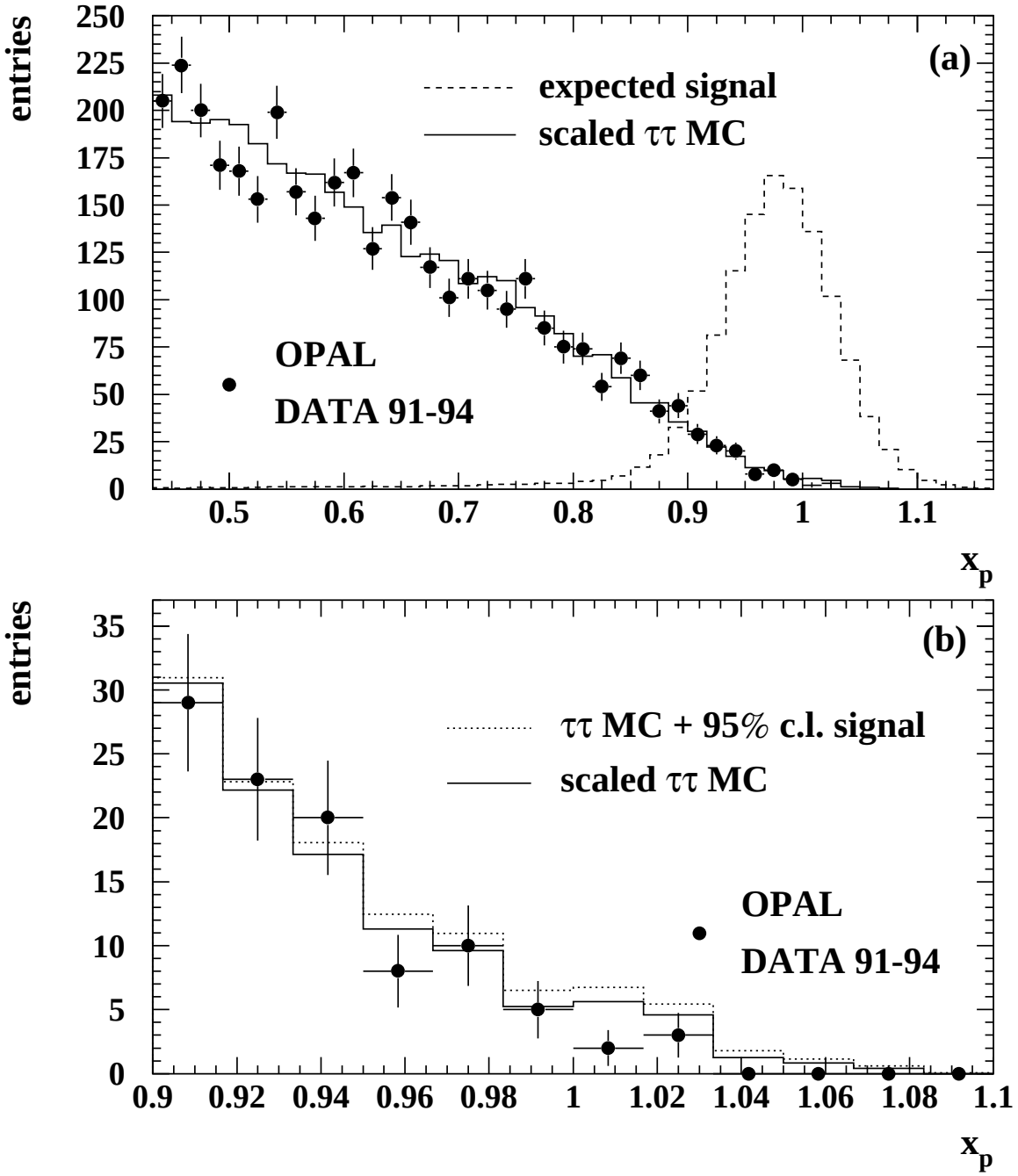

Figure 7: *Distribution of x_p of the muon candidates after all cuts for the $\mu\tau$ selection in data (dots), in $Z^0 \to \tau^+\tau^-$ Monte Carlo (histogram) and the shape of the expected signal of muon cones from tagged $Z^0 \to \mu^+\mu^-$ data events (dashed line). In (a) the entire x_p distribution is shown, while in (b) the interesting region around $x_p = 1$ is shown. The level of the signal shape is arbitrary in (a), while in (b) the $Z^0 \to \tau^+\tau^-$ Monte Carlo plus the 95% c.l. signal is shown as the dotted histogram.*

Fig. 8

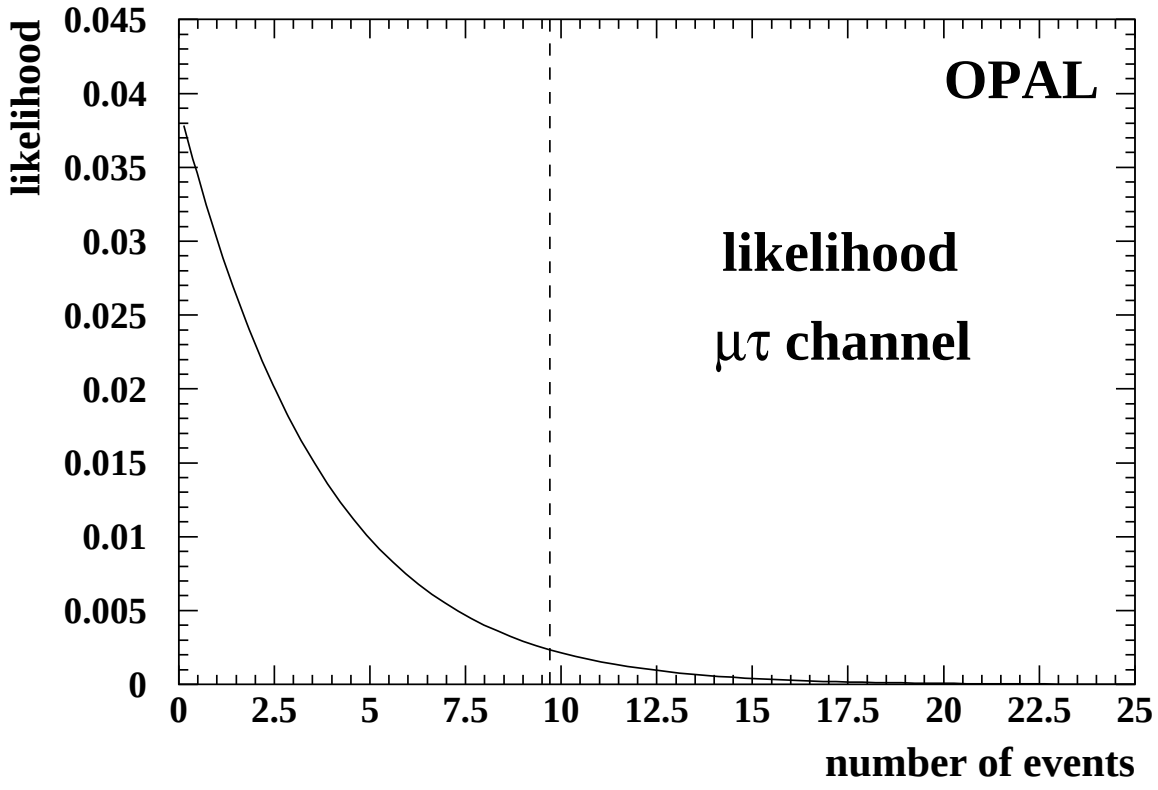

Figure 8: *Likelihood as a function of the number of $\mu\tau$ events in the data sample for 60 bins. The dashed line corresponds to the 95% c.l. limit on the number of* $Z^0 \rightarrow \mu\tau$ *events.*

Fig. 9

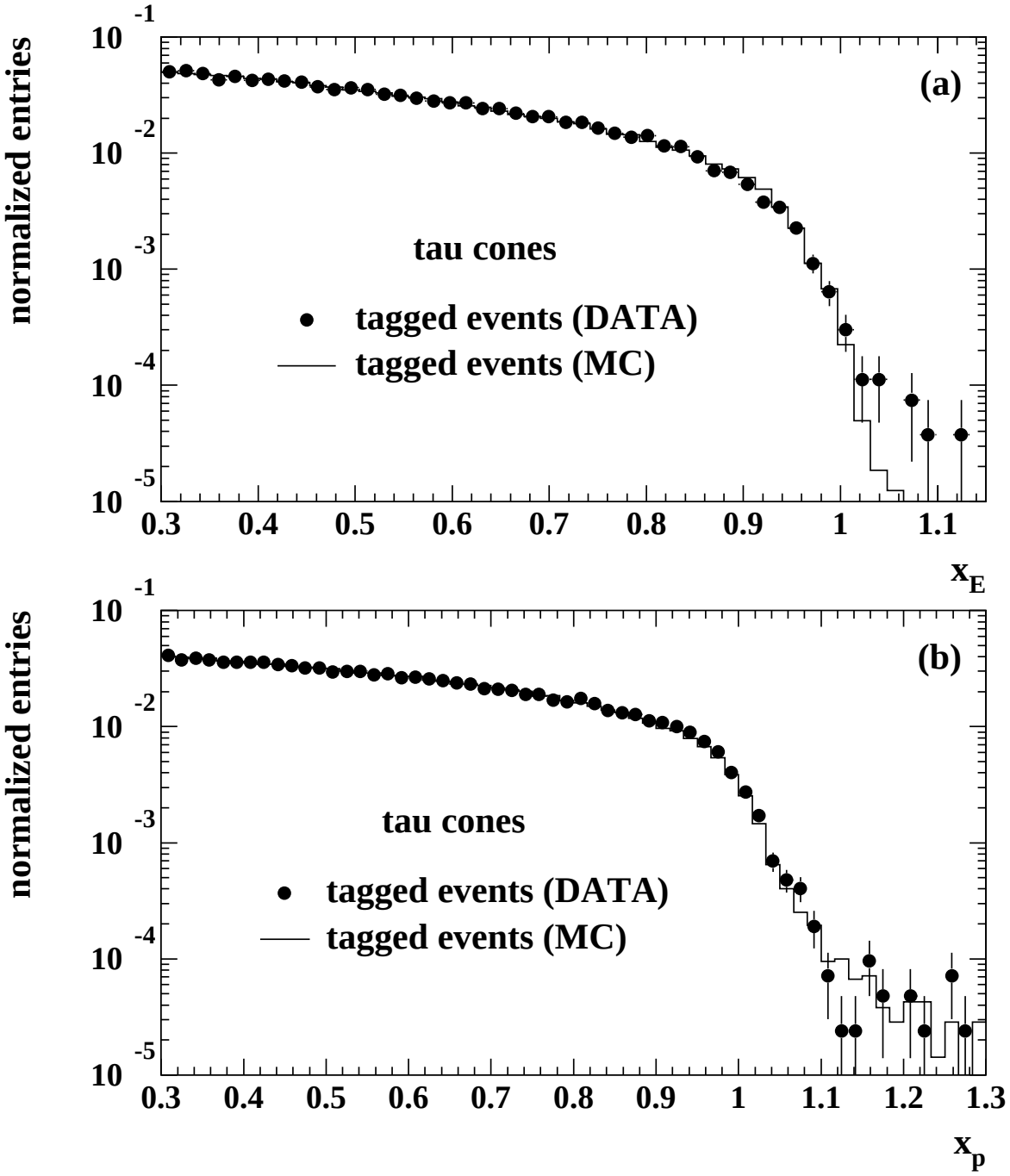

Figure 9: *Energy distribution (a) and momentum distribution (b) of tagged* $Z^0 \rightarrow \tau^+\tau^-$ *events. The Monte Carlo expectations are given as histograms and the data distributions as dots.*